Molecular Crystals and Liquid Crystals

Publication details, including instructions for authors and subscription information:
http://www.tandfonline.com/loi/gmcl20

Synthesis and Characterization of Some New Mesogenic Schief Base Esters N-[4-(4-n-Hexadecanoyloxybenzoyloxy)-Benzylidene]-4-Substituted Anilines

Guan-Yeow Yeap [a], Sie-Tiong Ha [a], Peng-Lim Boey [a], Wan Ahmad Kamil Mahmood [a], Masato M. Ito [b] & Yamashita Youhei [b]

[a] Liquid Crystal Research Laboratory, School of Chemical Sciences, Universiti Sains Malaysia, Penang, Malaysia

[b] Department of Environmental Engineering for Symbiosis, Faculty of Engineering, Soka University, Tokyo, Japan

Version of record first published: 31 Aug 2006

To cite this article: Guan-Yeow Yeap, Sie-Tiong Ha, Peng-Lim Boey, Wan Ahmad Kamil Mahmood, Masato M. Ito & Yamashita Youhei (2006): Synthesis and Characterization of Some New Mesogenic Schief Base Esters N-[4-(4-n-Hexadecanoyloxybenzoyloxy)-Benzylidene]-4-Substituted Anilines, Molecular Crystals and Liquid Crystals, 452:1, 73-90

To link to this article: http://dx.doi.org/10.1080/15421400500382156

Mol. Cryst. Liq. Cryst., Vol. 452, pp. 73–90, 2006

ISSN: 1542-1406 print/1563-5287 online
DOI: 10.1080/15421400500382156

Synthesis and Characterization of Some New Mesogenic Schief Base Esters *N*-[4-(4-*n*-Hexadecanoyloxybenzoyloxy)-Benzylidene]-4-Substituted Anilines

Guan-Yeow Yeap
Sie-Tiong Ha
Peng-Lim Boey
Wan Ahmad Kamil Mahmood
Liquid Crystal Research Laboratory, School of Chemical Sciences, Universiti Sains Malaysia, Penang, Malaysia

Masato M. Ito
Yamashita Youhei
Department of Environmental Engineering for Symbiosis, Faculty of Engineering, Soka University, Tokyo, Japan

Series of elongated Schiff base esters containing three aromatic rings with palmitoyl moiety as one of the terminal carbon chain and various substituents R(R=H, F, Cl, Br, OCH_3, CH_3, and C_2H_5) at the other end of molecule have been isolated, and their structures were proposed via physical measurement. The mesomorphic properties of these compounds were investigated via differential scanning calometry and polarizing optical microscopy. The thermal data indicate that all of these compounds exhibit mesomorphic properties. Although compounds with R=H, OCH_3, CH_3, and C_2H_5 show nematic phases, the remaining compounds containing halogen F, Cl, and Br are smectogenic in nature. The structural changes that result in the variation of transition temperature and the electronic polarizability of the respective molecules are discussed.

Keywords: electronic polarizability; elongated Schiff base esters; mesomorphic properties; palmitonyl; transition temperature

Address correspondence to Guan-Yeow Yeap, Liquid Crystal Research Laboratory, School of Chemical Sciences, Universiti Sains Malaysia, Penang, Malaysia. E-mail: gyyeap@usm.my or gyyeap_liqcryst_usm@yahoo.com

INTRODUCTION

Compounds containing two unsaturated rings with terminal substituents or multiple substituents are low-mass molecules capable of exhibiting mesomorphic properties [1]. The typical examples of these compounds are Schiff base esters, made up of an ester linkage at one terminal and different substituents residing at the other end along the long molecular axis. Over the past few years, the studies of the low-molar-mass liquid crystals comprising Schiff base esters have been documented, wherein the influence of terminal alkyl chain upon the mesomorphic properties [2,3] and the possibility of enhancing the rigidity of the core system of Schiff bases through metal complex formation [4–6] have been claimed as essential ways to enhance the mesomorphic properties.

In our present laboratory, an extensive study on the Schiff base ester *p*-n-alkanoyloxybenzylidene-*p*-substituted-anilines, which possess two aromatic rings, has been carried out in which the effect of mesomorphic properties arising from the different substituents (H, CH_3, OCH_3, Cl, CN, NO_2, OH, and COOH) was reported [7,8]. Through these studies, it has been revealed that compounds possessing polar OH and COOH substituents showed a tendency to exhibit smectic C rather than smectic A phases. Subsequent study of the *o*-n-hydroxy-*p*-n-alkanoyloxybenzylidene-*p*-substituted-anilines has disclosed that the rigidity of the core system in these Schiff base esters could be enhanced through the introduction of the lateral hydroxy group into the aldehyde fragment [9]. It has been claimed that the introduction of a lateral polar hydroxy group increased the molecular polarizability as well as the clearing temperature.

To further enhance the molecule length–breadth ratio of these Schiff base esters, we introduced an aromatic ring into the aldehyde fragment of the existing core system. The new compounds reported here are *N*-4-[4-(4-*n*-hexadecanoyloxybenzoyloxy)benzylidene]-R-anilines, in which R is H, F, Cl, Br, OCH_3, CH_3, and C_2H_5. Elemental analysis, mass spectrometry, FT-IR, and ^1H and ^{13}C NMR spectroscopic studies support the proposed structure, and polarizing optical microscopy (POM) and differential scanning calorimetry (DSC) confirmed the presence of liquid crystal properties for all the title compounds.

EXPERIMENTAL

Reagents and Techniques

4-Cloroaniline, 4-bromoaniline 4-ethylaniline, 4-hydroxybenzoic acid, and 4-dimethylaminopyridine (DMAP) were obtained from Merck (Germany). Aniline was purchased from BDH (England). 4-Hydroxybenzaldehyde,

4-fluoroaniline, and dicyclohexylcarbodiimide (DCC) were purchased from Acros Organics (USA), and 4-methoxyaniline was obtained from Fluka Chemie (Switzerland). 4-Methylaniline was purchased from Rieden-de-Haen (Germany).

Analyses were performed on 2400 LS series CHNS/O analyzers. Electron impact mass spectra (EI-MS) data were recorded by a Hewlett Packard 5989A mass spectrometer operating at 70-eV ionizing energy. Samples were introduced by using a direct inlet system with a source temperature of 200°C. IR data were recorded on a Perkin Elmer 2000-FTIR spectrophotometer in the frequency range 4000–400 cm^{-1} with samples embedded in KBr discs. NMR spectra were recorded in $CDCl_3$ at 298 K on a Bruker 400-MHz ultrashield spectrometer equipped with a 5-mm broad band inverse (BBI) gradient probe. Standard Bruker pulse programs [10] were used throughout the entire experiment. The complete ^1H and ^{13}C NMR assignments of representative compounds were obtained and substantiated by means of $^1H-^1H$ correlation spectroscopy (COSY), $^{13}C-^1H$ heteronuclear multiple quantum correlation (HMQC), and $^{13}C-^1H$ heteronuclear multiple bond correlation (HMBC) correlation spectroscopic measurements as described in the literature [11,12]. Thin-layer chromatography analyses were performed using aluminium-backed silica-gel plates (Merck 60 F254) and were examined under shortwave UV light.

The phase-transition temperatures for the compounds were determined using differential scanning calorimetry on a Schidmadzu DSC-50, which adopts a scanning rate of 20°C min^{-1}. The thermal behavior was studied via the enthalpy values expressed in kJ mol^{-1}. A polarizing microscope (Carl Zeiss) equipped with a heating stage (Metler FP52) was used for temperature-dependent study of liquid crystal textures. A video camera (Video Master coomo20P) installed on the polarizing microscope was coupled with a video capture card (Video Master coomo600), allowing real-time video capture and image saving. Phase identification was made by comparing the observed texture with those reported in the literature [13].

A molecular modeling study was performed using ACD/Chemsketch Version 4.5. Geometrical optimization or energy minimization of the molecules was performed to gain an appreciation of molecular shape and geometry. The structural conformation obtained was subsequently used in calculating the polarizability of each compound as reported earlier [9].

Synthesis

Synthesis of 4-n-Hexadecanoyloxybenzoic Acid

4-Hydroxybenzoic acid (10 mmol) and 5 ml of triethylamine were added to 50 mL of dichloromethane (CH_2Cl_2), and the solution was

heated until all substances completely dissolved. To this solution, 13 mmol of palmitoyl chloride was added and refluxed with stirring for 5 h. The reaction was performed under a constant flow of nitrogen gas. Finally, the reaction mixture was filtered, and CH_2Cl_2 was removed from the filtrate by evaporation. The white solid thus obtained was recrystallized twice with chloroform. Yield 56%. IR (KBr): ν_{max}/cm^{-1} 2952, 2918, 2849 (C−H aliphatic), 1755 (C=O of $C_{15}H_{31}COO-$fragment), 1682 (C=O of COOH).

Synthesis of 4-(4-n-Hexadecanoyloxybenzoyloxy) benzaldehyde, 1

To the 4-n-hexadecanoyloxybenzoic acid (5 mmol), an excess of thionyl chloride (25 ml) was added, and the mixture was heated under reflux for 3 h. The hot solution was then evaporated to dryness, and the resulting solid was dissolved in dry dichloromethane (40 ml). To this, 4-hydrozybenxaldehyde (5 mmol) dissolved in 5 ml of DMF was added. The mixture was stirred and heated under reflux for 5 h under nitrogen gas. Finally, the reaction mixture was filtered and dichloromethane removed from the filtrate by evaporation; the DMF solvent in the wet residue was removed by filtration using a Buchner funnel. The remaining starting material (4-hydroxybenzaldehyde) was easily removed together with the DMF solvent. The grey solid **1** thus obtained was recrystallized several times with methanol whereupon the pure compound was formed. Yield 34%. Found: C, 75.23; H, 8.28; calc. for $C_{30}H_{40}O_5$; C, 74.97; H, 8.39%. IR (KBr): ν_{max}/cm^{-1} 2954, 2917, 2849 (C−H aliphatic), 1756 (C=O of benzoate), 1743 (C=O of $C_{15}H_{31}COO-$fragment), 1701 (C=O of aldehyde).

Synthesis of Schiff Bases N-4-[4-(4-n-Hexadecanoyloxybenzoyloxy)benzylidene]-4-substituted Anilines, 9–15

The molecular structure of Schiff bases **9–15** are shown in Scheme 1. The Schiff bases were synthesized by mixing equimolar amounts of compound **1** with the appropriate anilines, both dissolved in absolute ethanol. The reaction mixture was refluxed for 3 h with stirring before it was filtered. The solvent was removed from the filtrate by evaporation. The light yellowish crystals of **9–15** thus obtained were recrystallized from ethanol until constant transition temperatures were attained. The entire synthetic route is outlined in Scheme 1. The elemental analysis and EI-MS data of all compounds are listed in Table 1. The IR, ^1H NMR, and ^{13}C NMR spectral data of all the compounds are summarized as follows.

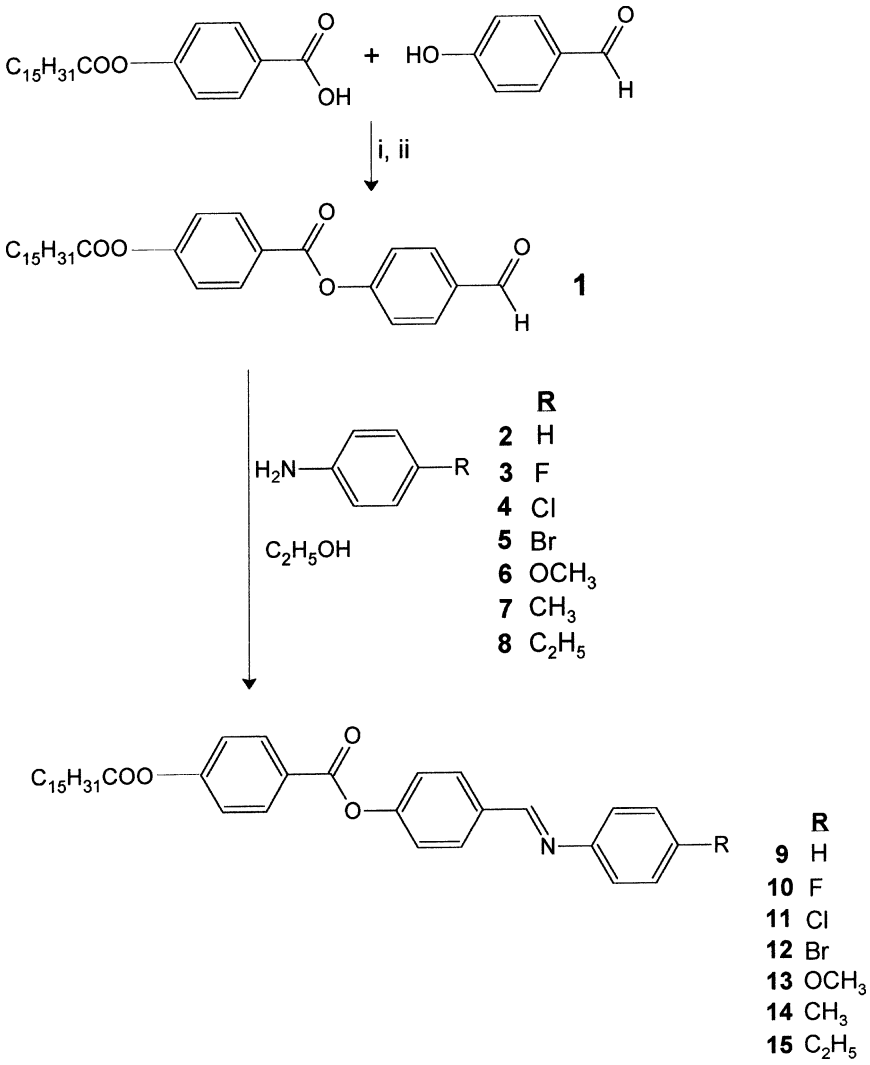

SCHEME 1 Synthetic routes toward the formation of intermediates and target compounds **12–21**. Reagent and conditions: (i) $SOCl_2$ reflux for 3 h; (ii) anhydrous CH_2Cl_2, DMF, $(C_2H_5)_3N$, N_2 atmosphere, reflux for 5 h.

Data

Compound **9**: Yield 37%. IR (KBr): υ_{max}/cm^{-1} 2952, 2918, 2849 (C–H aliphatic), 1745 (C=O of $C_{15}H_{31}COO-$ fragment), 1732 (C=O of benzoate), 1625 (C=N), 1602 (C=C aromatic), 1280 (C–O). ^1H NMR (400 MHz, $CDCl_3$): δ 0.87–0.90 (t, 3H, $C\underline{H}_3-CH_2-$), 1.28–1.43

TABLE 1 Physical Data of Schiff Bases **9–15**

Compound	Formula	Molecular weight	M^+ (relative intensity %)	% Required (% found)		
				C	H	N
9	$C_{36}H_{45}NO_4$	555.75	555.65 (1)	77.80 (77.89)	8016 (8.13)	2.52 (2.55)
10	$C_{36}H_{44}NO_4F$	573.74	573.55 (>1)	75.36 (75.41)	7.73 (7.69)	2.44 (2.40)
11	$C_{36}H_{44}NO_4Cl$	590.19	590.15 (>1)	73.26 (73.21)	7.51 (7.55)	2.37 (2.35)
12	$C_{36}H_{44}NO_4Br$	634.64	634.55 (1)	68.13 (68.09)	6.99 (7.01)	2.21 (2.27)
13	$C_{37}H_{47}NO_5$	585.77	585.35 (1)	75.86 (75.95)	8.09 (8.13)	2.39 (2.34)
14	$C_{37}H_{47}NO_4$	569.77	569.65 (1)	78.00 (77.97)	8.31 (8.33)	2.46 (2.45)
15	$C_{38}H_{49}NO_4$	583.80	583.65 (>1)	78.18 (78.25)	8.46 (8.50)	2.40 (2.33)

(m, 24H, $CH_3-(CH_2)_{12}-C_2H_4COO-$), 1.77–1.82 (m, 2H, $-CH_2-CH_2COO-$), 2.59–2.64 (t, 2H, $-CH_2-COO-$), 7.23–7.29 (m, 5H, Ar−H), 7.34–7.45 (m, 4H, Ar−H), 7.98–8.02 (dd, 2H, Ar−H), 8.25–8.28 (dd, 2H, Ar−H), 8.49 (s, 1H, CH=N). ^{13}C NMR (100 MHz, $CDCl_3$): 172.09 (C=O of $C_{15}H_{31}COO-$), 164.48 (C=O of benzoate), 159.51 (C=N), 153.61, 134.45, 132.36, 132.31, 132.25, 130.47, 129.58, 127.03, 126.45, 122.57, 122.50, 122.44, 122.36, and 126.45 for aromatic carbons, 34.82, 32.32, 30.08, 30.06, 29.99, 29.85, 29.76, 29.65, 29.49, 25.25, 23.10, and 14.53 for carbons in the alkyl chain ($C_{15}H_{31}COO-$).

Compound **10**: Yield 55%. IR (KBr): ν_{max}/cm^{-1} 2951, 2920, 2851 (C−H aliphatic), 1746 (C=O of $C_{15}H_{31}COO-$ fragment), 1733 (C=O of benzoate), 1627 (C=N), 1602 (C=C aromatic), 1279 (C−O). ^{1}H NMR (400 MHz, $CDCl_3$): δ 0.90–0.93 (t, 3H, CH_3-CH_2-), 1.24–1.47 (m, 24H, $CH_3-(CH_2)_{12}-C_2H_4COO-$), 1.77–1.84 (m, 2H, $-CH_2-CH_2COO-$), 2.60–2.64 (t, 2H, $-CH_2-COO-$), 7.08–7.15 (m, 2H, Ar−H), 7.21–7.25 (m, 2H Ar−H), 7.27–7.31 (m, 2H, Ar−H), 7.36–7.38 (m, 2H, Ar−H), 7.98–8.01 (dd, 2H, Ar−H), 8.25–8.27 (dd, 2H, Ar−H), 8.48 (s, 1H, CH=N). ^{13}C NMR (100 MHz, $CDCl_3$): 171.87 (C=O of $C_{15}H_{31}COO$), 164.36 (C=O of benzoate), 159.05 (C=N), 160.53, 155.65, 153.76, 143.38, 134.39, 132.16, 130.37, 127.10, 122.70, 122.50, 122.27, and 116.12 for aromatic carbons, 34.81, 32.37, 30.03, 30.01, 29.98, 29.93, 29.79, 29.68, 29.58, 29.46, 25.23, 23.01, and 14.37 for carbons in the alkyl chain ($C_{15}H_{31}COO-$).

Compound **11**: Yield 62%. IR (KBr): ν_{max}/cm^{-1} 2950, 2919, 2851 (C−H aliphatic), 1745 (C=O of $C_{15}H_{31}COO-$ fragment), 1733 (C=O of benzoate), 1625 (C=N), 1601 (C=C aromatic), 1280 (C−O). ^{1}H NMR (400 MHz, $CDCl_3$): δ 0.91–0.94 (t, 3H, CH_3-CH_2-), 1.32–1.47 (m, 24H, $CH_3-(CH_2)_{12}-C_2H_4COO-$), 1.78–1.83 (m, 2H, $-CH_2-CH_2COO-$), 2.61–2.64 (t, 2H, CH_2-COO-), 7.17–7.19 (d, 2H, Ar−H), 7.28–7.30 (d, 2H, Ar−H), 7.37–7.40 (m, 4H, Ar−H), 7.99–;8.01 (dd, 2H,

Ar−H), 8.25–8.27 (dd, 2H, Ar−H), 8.47 (s, 1H, CH=N). ^{13}C NMR (100 MHz, $CDCl_3$): 171.83 (C=O of $C_{15}H_{31}COO-$), 164.32 (C=O of benzoate), 159.58 (C=N), 155.68, 153.92, 150.82, 134.28, 132.16, 132.06, 130.48, 129.63, 127.09, 122.61, 122.53, and 122.27 for aromatic carbons, 34.82, 32.26, 30.01, 29.98, 29.93, 29.78, 29.67, 29.57, 29.46, 25.23, 22.99, and 14.35 for carbons in the alkyl chain ($C_{15}H_{31}COO-$).

Compound **12**: Yield 60%. IR (KBr): v_{max}/cm^{-1} 2949, 2916, 2848 (C−H aliphatic), 1745 (C=O of $C_{15}H_{31}COO-$ fragment), 1733 (C=O of benzoate), 1623 (C=N), 1602 (C=C aromatic), 1279 (C−O). ^{1}H NMR (400 MHz, $CDCl_3$): δ 0.87–0.90 (t, 3H, CH_3-CH_2-), 1.28–1.43 (m, 24H, $CH_3-(CH_2)_{12}-C_2H_4COO-$), 1.77–1.82 (m, 2H, $-CH_2-CH_2COO-$), 2.59–2.64 (t, 2H, $-CH_2-COO-$), 7.11–7.13 (d, 2H, Ar−H), 7.28–7.33 (d, 2H, Ar−H), 7.37–7.39 (d, 2H, Ar−H), 7.53–7.56 (dd, 2H, Ar−H), 7.98–8.00 (dd, 2H, Ar−H), 8.25–8.27 (dd, 2H, Ar−H), H), 8.46 (s, 1H, CH=N). ^{13}C NMR (100 MHz, $CDCl_3$): 172.05 (C=O of $C_{15}H_{31}COO-$), 164.42 (C=O of benzoate), 159.83 (C=N), 155.60, 153.84, 151.25, 134.18, 132.64, 132.25, 130.57, 126.99, 123.01, 122.64, 122.37, and 119.84 for aromatic carbons, 34.83, 32.34, 30.11, 30.06, 30.01, 29.87, 29.77, 29.66, 29.50, 25.25, 23.10, and 14.53 for carbons in the alkyl chain ($C_{15}H_{31}COO-$).

Compound **13**: Yield 33%. IR (KBr): v_{max}/cm^{-1} 2953, 2916, 2848 (C−H aliphatic), 1742 (C=O of $C_{15}H_{31}COO-$ fragment), 1753 (C=O of benzoate), 1624 (C=N), 1605 (C=C aromatic), 1284 (C−O). ^{1}H NMR (400 MHz, $CDCl_3$): δ 0.88–0.92 (t, 3H, CH_3-CH_2-), 1.22–1.48 (m, 24H, $CH_3-(CH_2)_{12}-C_2H_4COO-$), 1.75–1.84 (m, 2H, $-CH_2-CH_2COO-$), 2.60–2.65 (t, 2H, $-CH_2-COO-$), 3.86 (s, 3H, $Ar-OCH_3$), 6.98–6.95 (d, 2H, Ar−H), 7.26–7.28 (dd, 4H, Ar−H), 7.33–7.36 (d, 2H, Ar−H), 7.97–8.00 (d, 2H, Ar−H), 8.25 (d, 2H, Ar−H), 8.52 (s, 1H, CH=N). ^{13}C NMR (100 MHz, $CDCl_3$): 172.10 (C=O of $C_{15}H_{31}COO-$), 164.50 (C=O of benzoate), 158.77 (C=N), 157.49, 153.33, 132.35, 132.31, 132.24, 130.21, 127.07, 122.62, 122.51, 122.44, 122.35, and 114.81 for aromatic carbons, 55.91 ($Ar-OCH_3$), 34.83, 32.33, 30.10, 30.09, 30.06, 30.00, 29.86, 29.77, 29.65, 29.50, 25.24, 23.10, and 14.53 for carbons in the alkyl chain ($C_{15}H_{31}COO-$).

Compound **14**: Yield 32%. IR (KBr): v_{max}/cm^{-1} 2952, 2916, 2848 (C−H aliphatic), 1745 (C=O of $C_{15}H_{31}COO-$ fragment), 1753 (C=O of benzoate), 1624 (C=N), 1605 (C=C aromatic), 1284 (C−O). ^{1}H NMR (400 MHz, $CDCl_3$): δ 0.89–0.93 (t, 3H, CH_3-CH_2-), 1.29–1.48 (m, 24H, $CH_3-(CH_2)_{12}-C_2H_4COO-$), 1.75–1.85 (m, 2H, $-CH_2-CH_2COO-$), 2.41 (s, 1H, $AR-CH_3$), 2.60–2.65 (t, 2H, $-CH_2-COO-$), 7.17–7.43 (m, 8H, Ar−H), 7.99–8.02 (dd, 2H, Ar−H), 8.25–8.30 (m, 2H, Ar−H), 8.51 (s, 1H, CH=N). ^{13}C NMR (100 MHz, $CDCl_3$): 172.08 (C=O of $C_{15}H_{31}COO-$), 164.48 (C=O of benzoate), 158.67 (C=N), 153.48,

136.34, 132.35, 132.31, 132.24, 130.36, 130.20, 127.07, 122.52, 122.44, 122.35, and 121.24 for aromatic carbons, 21.43 (Ar−$\underline{C}H_3$), 34.83, 32.34, 30.11, 30.07, 30.06, 30.01, 29.87, 29.78, 29.66, 29.50, 25.25, 23.11, and 14.54 for carbons in the alkyl chain ($\underline{C}_{15}H_{31}COO-$).

Compound **15**: Yield 31%. IR (KBr): υ_{max}/cm^{-1} 2953, 2916, 2848 (C−H aliphatic), 1745 (C=O of $C_{15}H_{31}COO-$ fragment), 1754 (C=O of benzoate), 1625 (C=N), 1603 (C=C aromatic), 1280 (C−O). ^{1}H NMR (400 MHz, $CDCl_3$): δ 0.89–0.93 (t, 3H, $\underline{C}H_3-CH_2-$), 1.25–1.28 (t, 3H, Ar−$CH_2-\underline{C}H_3$), 1.29–1.46 (m, 24H, $CH_3-(\underline{C}H_2)_{12}-C_2H_4COO-$), 1.77–1.84 (m, 2H, $-\underline{C}H_2-CH_2COO-$), 2.61–2.65 (t, 2H, $-\underline{C}H_2-COO-$), 2.68–2.74 (q, 2H, Ar−C $\underline{H}_2-CH_3$), 7.19–7.22 (m, 2H, Ar−H), 7.25–7.29 (m, 4H, Ar−H), 7.35–7.37 (d, 2H, Ar−H), 7.99–8.02 (dd, 2H, Ar−H). 8.26–8.28 (dd, 2H, Ar−H), 8.51 (s, 1H, CH=N). ^{13}C NMR (100 MHz, $CDCl_3$): 172.09 (C=O of $C_{15}H_{31}\underline{C}OO-$), 164.49 (C=O of benzoate), 158.72 (C=N), 153.48, 134.63, 132.36, 132.31, 132.25, 130.37, 129.00, 127.08, 122.52, 122.45, 122.35, and 121.30 for aromatic carbons, 28.85 (Ar−$\underline{C}H_2CH_3$), 16.05 (Ar−$\underline{C}H_2\underline{C}H_3$), 34.83, 32.33, 30.09, 30.06, 30.00, 29.86, 29.77, 29.65, 29.50, 25.25, 23.10, and 14.53 for carbons in the alkyl chain ($\underline{C}_{15}H_{31}COO-$).

RESULTS AND DISCUSSION

Structure identification of compounds **9–15** was established on the basis of the elemental analysis, mass spectrometric, and spectroscopic methods (FT-IR and NMR). The percentages of C, H, and N from the elemental analysis conform with the calculated values for compounds **9–15** as shown in Table 1. Mass spectra of compounds **9–15** were studied by electron impact ionization. The molecular ion peak obtained from the experimental for the title compounds (Table 1) are in good agreement with the theoretical values. The representative EI mass spectra of **13** and **14** are shown in Fig. 1.

FT-IR, ^{1}H, NMR, and ^{13}C NMR Spectral Studies

FT-IR, ^{1}H NMR, and ^{13}C NMR spectroscopic techniques were used for confirming the structure of all the title compounds. The FT-IR spectra of compounds **9–15** show the absorption bands assignable to the stretching of aliphatic C−H at the frequency range of 2848–2953 cm^{-1}. The band appears at the frequency range of 1623–1627 cm^{-1} can be ascribed to the stretching of C=N bond of compounds **9–15**, and these values conform with those reported in

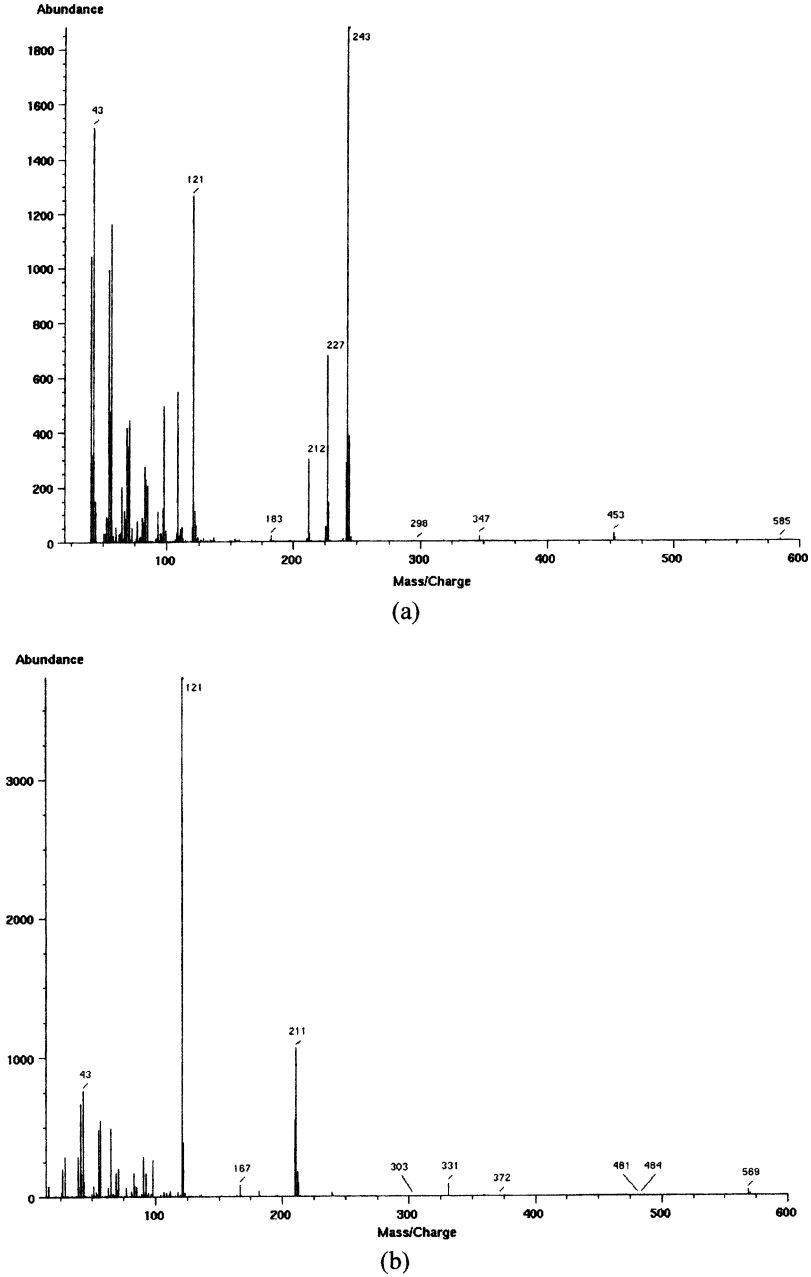

FIGURE 1 Electron impact mass spectra of (a) compound **13** and (b) compound **14**.

the IR spectra for various substituted aromatic Schiff bases that possess a general formulation $C_6H_5CH{=}NC_6H_5$ [7,9]. For compound **9**, the appearance of two C=O bands at 1745 and 1732 cm^{-1} can be ascribed to the respective ester carbonyl of $C_{15}H_{31}COO-$ fragment and benzoate Ar−COO− group. Compounds **10–15** show the similar characteristic bands as discussed for compound **9**. The representative IR spectra of compounds **9**, **10**, **12**, and **13** are shown in Fig. 2.

^{1}H NMR data of compounds **9–12** show the presence of a singlet peak assigned to the azomethine proton (CH=N) at the chemical shift $\delta = 8.46$–8.52 ppm. Compound **9** shows two triplets assignable to the methyl (CH_3) group of ester linkage and $-C\underline{H}_2-COO-$ protons at $\delta = 0.87$–0.90 and 2.64 ppm, respectively. The other methylene protons of $CH_3-(C\underline{H}_2)_{12}-C_2H_4COO-$ group and $-C\underline{H}_2-CH_2COO-$ group in the alkyl chain were confirmed by the presence of two multiplet signals at the respective chemical shift $\delta = 1.28$–1.43 and 1.77–1.82 ppm. The ^{1}H NMR spectrum of compound **9** also shows the presence of 12 aromatic protons within the range of $\delta = 7.23$–8.28 ppm. The peaks with similar characteristics were also observed for compounds **10–15**. The resonance owing to the aromatic H atoms in the aniline fragment of compounds **9–15** appeared at different chemical shifts and showed different splitting in each compound. This observation can be due to the presence of different *para*-substituents (H, F, Cl, Br, OCH_3, CH_3, and C_2H_5), which results in the different chemical

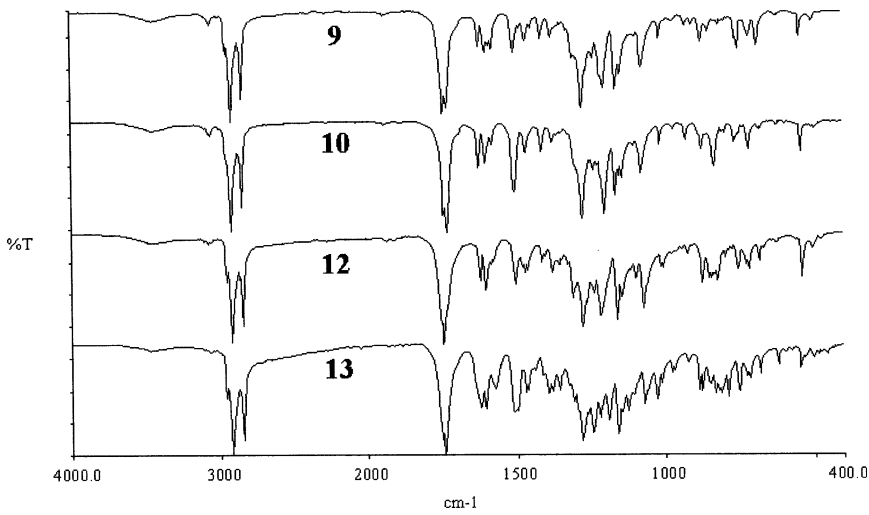

FIGURE 2 FT-IR spectra of compounds **9**, **10**, **12**, and **13**.

environment. As a representative case, the complete ^{1}H NMR assignment of compound **12** was carried out with the aid of a two-dimensional ^{1}H-^{1}H COSY experiment. Figure 3 showed the structural assignment and ^{1}H NMR spectrum of compound **12**. For compound **14**, an additional peak occurring at $\delta = 2.41$ ppm can be attributed to the presence of methyl group (Ar$-$CH$_3$) in the aniline fragment. In the ^{1}H NMR spectrum of compound **15**, two additional peaks assignable to the methyl protons and methylene protons of the ethyl group attached to the aniline fragment (Ar-CH$_2$CH$_3$) were observed at the respective chemical shift $\delta = 1.25$–1.28 and 2.68–2.74 ppm. An additional peak occurring at $\delta = 3.86$ ppm can be attributed to the presence of the methoxy (OCH$_3$) group in compound **13**.

The molecular structures of the title compounds were further substantiated by ^{13}C NMR spectroscopy. The appearance of azomethine proton was evident based on the presence of a peak at $\delta = 159.51$ ppm ppm (compound **9**), $\delta = 159.05$ ppm (compound **10**), $\delta = 159.58$ ppm (compound **11**), $\delta = 159.83$ ppm (compound **12**), $\delta = 158.77$ ppm (compound **13**), $\delta = 158.67$ ppm (compound **14**), and $\delta = 158.72$ ppm (compound **15**). In the ^{13}C NMR spectrum of compound **9**, two different types of carbonyl carbons (COO$-$) signals occurring at $\delta = 172.09$ ppm

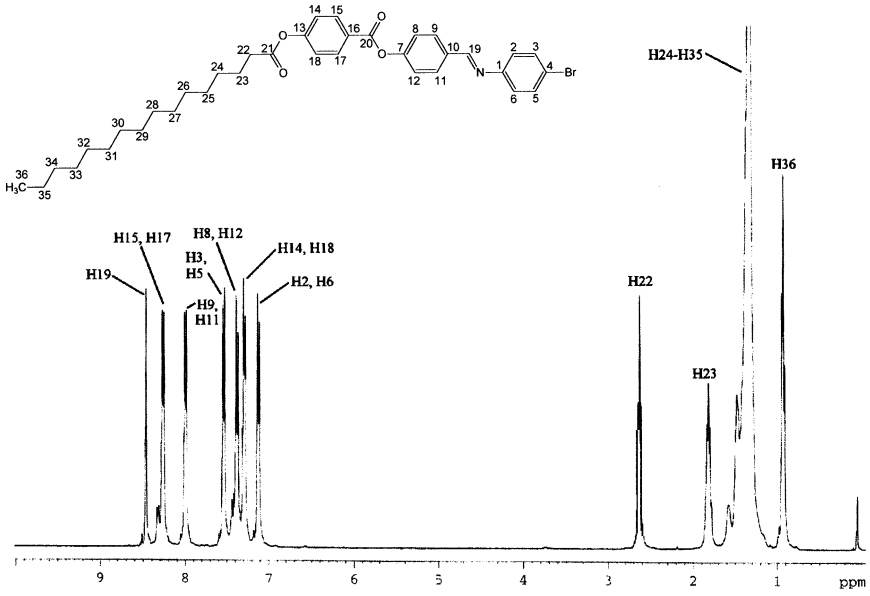

FIGURE 3 ^{1}H NMR spectrum and structural assignment of compound **12**.

and 164.48 ppm were attributed to the ester carbonyl of $C_{15}H_{31}COO-$ fragment and benzoate (Ar–COO–) group, respectively. The peaks with similar characteristics were also observed for compounds **10–15**. A representative ^{13}C NMR spectrum and complete structural assignment of compound **12** is shown in Fig. 4. The type of ^{13}C nuclei was determined by distortionless enhancement by polarization transfer (DEPT), and the ^{13}C assignments were deduced from HMQC experiments. From HMQC, CH_3, CH_2, and CH were assigned unambiguously.

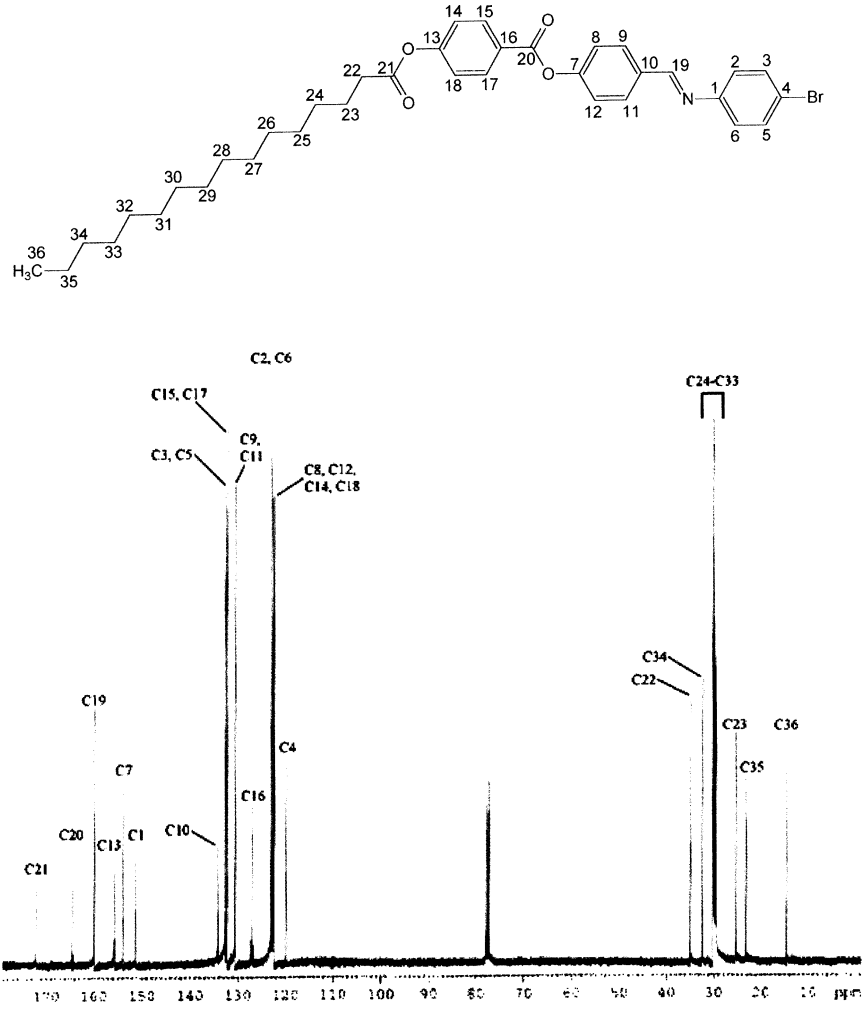

FIGURE 4 ^{13}C NMR spectrum and structural assignment of compound **12**.

The remaining signals attributable to the quaternary carbons were derived from HMBC correlations.

The results as inferred from the IR and NMR spectral data of all the compounds were found to be consistent with the proposed structure (Scheme 1).

Optical and Thermal Studies

All the compounds synthesized in the present study have been characterized using polarizing optical microscope (POM) and differential scanning calorimetry (DSC). Figure 5 shows the representative DSC thermograms of compounds **10–12**. Table 2 shows the phase transition temperatures, associated enthalpy (ΔH), and molar entropy (ΔS) values of all the compounds. Table 2 clearly shows that upon heating all compounds exhibit endotherms characteristic of the crystal–mesophase and mesophase–isotropic transitions at temperature greater than melting temperature (T_m). The enthalpy values also indicate the crystal–mesophase and mesophase–isotropic transitions in all the compounds **9–15**. Observation under crossed polarizers of compounds **9**, **13**, **14**, and **15** during the melting process showed schlieren threaded or marble texture typical of a nematic mesophase. Figure 6a

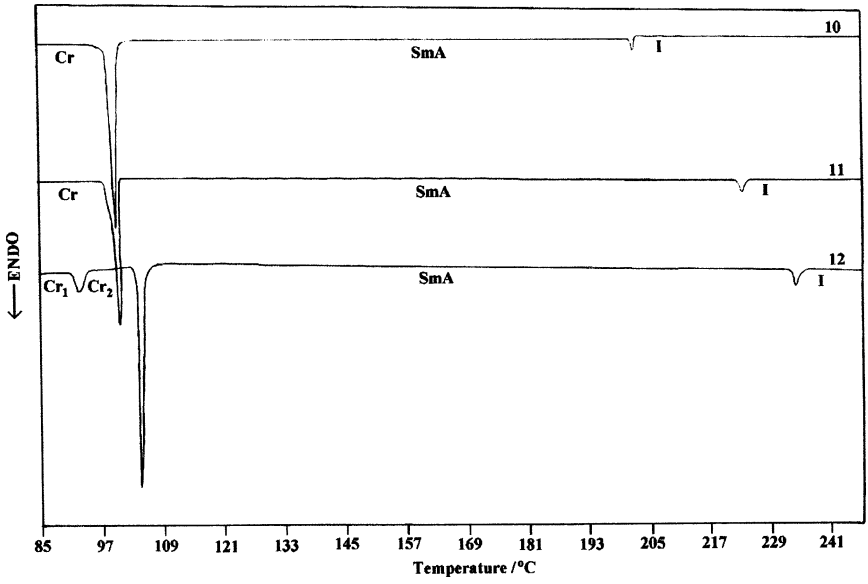

FIGURE 5 DSC thermograms of compounds **10–12** during heating scan.

TABLE 2 Transition Temperatures, Associated Enthalpy, and Entropy Changes of Compound **9–15**

Compound	Transition[a]	T (°C)	ΔH (kJ mol^{-1})	ΔS (10^{-3}) (kJ k^{-1} mol^{-1})
9	Cr_1-Cr_2	84.1	2.2	6.2
	Cr_2-N	99.7	50.9	136.5
	N-I	171.5	0.7	1.6
10	Cr-SmA	99.7	48.9	131.2
	SmA-I	201.4	5.1	10.7
11	Cr-SmA	100.3	41.3	110.6
	SmA-I	223.0	6.6	13.3
12	Cr_1-Cr_2	92.2	18.7	51.2
	Cr_2-SmA	104.6	45.4	120.2
	SmA-I	232.3	8.8	17.4
13	Cr-N	113.8	56.1	145.0
	N-I	235.1[b]	—	—
14	Cr_1-Cr_2	93.3	42.4	115.8
	Cr_2-N	99.9	14.1	37.8
	N-I	214.5	0.7	1.4
15	Cr_1-Cr_2	75.2	16.7	48.0
	Cr_2-N	94.8	35.0	95.2
	N-I	203.2	0.7	1.5

[a]Cr_1 and Cr_2, crystal; SmA, smectic A; N, nematic; I, isotropic.
[b]Polarized optical microscopy data.

shows the representative optical photomicrograph of compound **15** exhibiting nematic phase with marble texture. Among all title compounds, compounds **9**, **12**, **14**, and **15** show an endotherm in the DSC thermogram (Table 2) before the crystal–mesophase transition at 84.1, 92.2, 93.3, and 75.2°C, repectively. The texture observed under the polarizing microscope is indicative of the presence of subphases within the crystal phase (Cr_1-Cr_2), which resembles the phenomena reported in our recent finding on ortho-hydroxy-para-alkyloxybenzylidene-para-substituted anilines [9].

The data in Table 2 have also shown that compounds **10–12**, which possess F, Cl, Br substituents, respectively, exhibit smectic A (SmA) phase. The SmA phase has been identified from optical textures in which regions of focal conic fan and homeotropic texture coexist [14]. A representative optical photomicrograph of compound **10** exhibiting SmA phase is shown in Fig. 6b. The appearance of SmA phase is found to conform with earlier reported Sciff base esters *o*-n-hydroxy-*p*-n-hexadecanoyloxybenzylidene-*p*-fluoroaniline (**1 6 B-F**), *o*-n-hydroxy-*p*-n-hexadecanoyloxybenzylidene-*p*-chloroaniline (**16 B-Cl**), and *o*-n-hydroxy-*p*-n-hexadecanoyloxybenzylidene-*p*-bromaniline (**16B-Br**) [9].

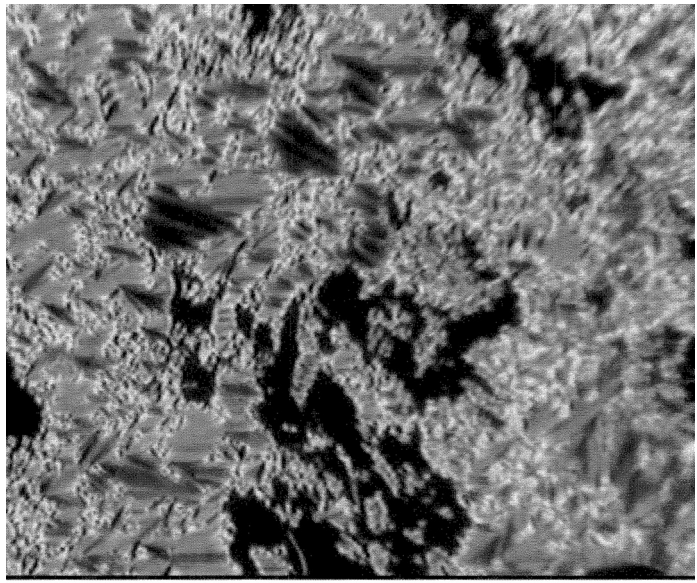

(a)

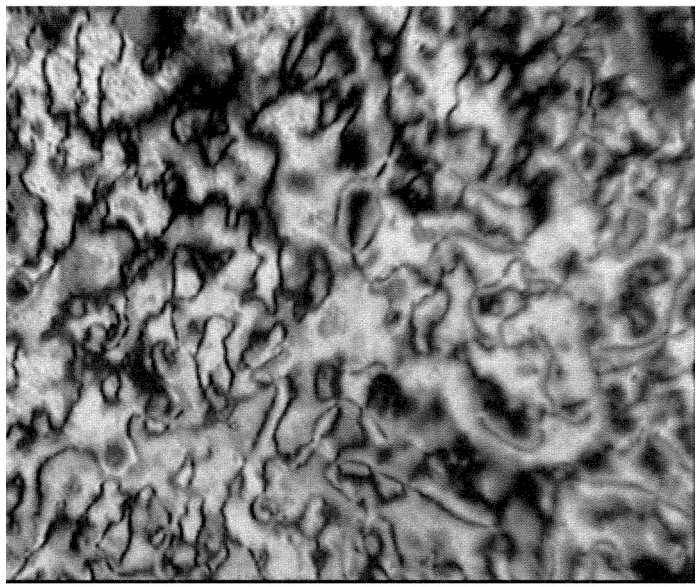

(b)

FIGURE 6 (a) Optical photomicrograph of compound **10** exhibiting smectic A with focal conic fan and homeotropic (dark area) textures; (b) optical photomicrography of compound **15** exhibiting nematic phase with marble textures.

Influence of Structural Changes on Mesomorphic Properties

The mesomorphic properties of compounds **9–15** were compared with the analogous compounds, *o*-n-hydroxy-*p*-n-hexadecanoyloxybenzylidene-X-substituted anilines (**16-X**), in which X is the substituent of H, F, Cl, Br, OCH_3, CH_3, and C_2H_5 [9]. Compounds **9–15** are found to be different from those reported analogous compounds owing to the presence of an additional aromatic ring joined to the benzylideneaniline core system via an ester bond. As such, it has been presumed to change the characteristic of the benzylideneaniline skeleton whereby the molecular length increases with little or no change in the width. These two factors allow an increase in the anisotropy of the molecule. Thus, the polarizability of molecules in compounds **9–15** is expected to rise. This has also been confirmed by the polarizability values wherein the calculated polarizability (Table 3) of compounds **9**, **10**, **11**, **12**, **13**, **14**, and **15** are higher than those values reported in the series of **16-X**: **16-H** $[(54.33 \pm 0.5) \times 10^{-24}\,cm^{-3}]$, **16-F** $[(54.28 \pm 0.5) \times 10^{-24}\,cm^{-3}]$, **16-Cl** $[(56.16 \pm 0.5) \times 10^{-24}\,cm^{-3}]$, **16 Br** $[(57.33 \pm 0.5) \times 10^{-24}\,cm^{-3}]$, **16-$OCH_3$** $[(56.64 \pm 0.5) \times 10^{-24}\,cm^{-3}]$, **16-$CH_3$** $[(56.09 \pm 0.5) \times 10^{-24}\,cm^{-3}]$, **16-$C_2H_5$** $[(57.09 \pm 0.5) \times 10^{-24}\,cm^{-3}]$, respectively [9]. As a consequence, the clearing temperature of compounds **9–15** is comparatively higher than those values reported for the analogous compounds [9].

Another important factor contributing to the difference in transition temperature from mesophase to isotropic phase is the influence of terminal group of X substituent in the present study. Among compounds **10–12** wherein each compound possesses the halogen in the aniline fragment, the clearing temperature for compound **10** is very much lower in comparison with **11** and **12** and can be represented by DSC thermograms upon heating scan in Fig. 5. This observation suggests that the fluorine (F) atom, which is the most electronegative,

TABLE 3 Polarizability (Calculated Value) for Compounds **9–15**

Compound	Polarizability ($\alpha \pm 0.5 \times 10^{-24}$)
9	66.66
10	66.61
11	68.49
12	69.66
13	68.97
14	68.42
15	70.24

reduces the degree of molecular order. It is apparent that the fluorine atom shows very low polarizability because the valence electrons residing at this atom are tightly held to the nucleus. However, the bromine atom is considered larger than fluorine and hence is more easily polarized because electrons on this atom are far from the nucleus [15]. This thermal data also indicates that the influence of steric hindrance due to the presence of the fluorine atom in compound **10**, which can be associated with the asymmetrical characteristic of the core system, is the least in comparison with compounds **11** and **12**, which possess larger Cl and Br atoms, respectively. As a result, the clearing temperatures of **11** and **12** will be higher than, that of compound **10**. This has also been confirmed by the polarizability values wherein the calculated polarizability follows the order of **10** < **11** < **12** (Table 3).

The nematic–isotropic transition temperature of compound **13** is 20°C higher than compound **14**, although both the compounds differ only slightly in the terminal substituent wherein compounds **13** and **14** possesses methoxy (OCH_3) and methyl (CH_3) moieties, respectively. This can be due to the oxygen of methoxy (OCH_3) group being in conjugation with the aromatic core, which, in addition to extending the length of the rigid core, enhances the polarizibility. This has been supported by the calculated polarizability values in which the polarizability of compound **13** is higher than compound **14** (Table 3). A similar phenomena was also observed for the analogous compounds, *o*-n-hydroxy-*p*-n-hexadecanoyloxybenzylidene-*p*-substituted-anilines (**16-X**) whereby the clearing temperature of **16-OCH$_3$** is 18°C higher than **16-CH$_3$** [9].

By comparing the mesophase–isotropic transition temperature (T_c) of compounds **9–15**, the following sequence can be established (compound are represented by its substituent).

T_c: H < F < C_2H_5 < CH_3 < Cl < Br < OCH_3.

ACKNOWLEDGMENT

G. Y. Yeap thanks Universiti Sains Malaysia, especially research creativity and management office (RCMO) and the Malaysian government, for the financial support through research grant 305/PKIMIA/612923. Partial financial funding through Open Research Project for year 2004–2005) granted by Soka University in Japan was also essential to accomplish this study. S. T. Ha is grateful to the Ministry of Science, Technology and Innovation of Malaysia for the National Science Fellowship award.

REFERENCES

[1] Jacobi, A. & Weissflog, W. (1997). *Liq. Cryst.*, *22*, 107.
[2] Dave, J. S. & Kurian, G. (1977). *Mol. Cryst. Liq. Cryst.*, *42*, 175.
[3] Matsunaga, Y. & Miyajima, N. (1990). *Mol. Cryst. Liq. Cryst.*, *178*, 157.
[4] Hoshino, N., Takashi, K., Sekuchi, T., Tanaka, H., & Matsunaga, Y. (1998). *Inorg. Chem.*, *37*, 882.
[5] Tian, Y., Su, F., Xing, P., Zhao, Y., Tang, X., Zhao, X., & Zhou, E. (1996). *Liq. Cryst.*, *20*, 139.
[6] Rao, N. V. S., Singha, D., Das, M., & Paul, M. K. (2002). *Mol. Cryst. Liq. Cryst.*, *373*, 105.
[7] Yeap, G. Y., Ooi, W. S., Nakamura, Y., & Cheng, Z. (2002). *Mol. Cryst. Liq. Cryst.*, *381*, 169.
[8] Ooi, W. S. (2003). M.Sc. Thesis, Universiti Sains Malaysia, Malaysia.
[9] Yeap, G. Y., Ha, S. T., Lim, P. L., Boey, P. L., Mahmood, W. A. K., Ito, M. M., & Sanehisa, S. (2004). *Mol. Cryst. Liq. Cryst.*, *423*, 73.
[10] Bruker program ID WIN-NMR (release 6.0) and 2D WIN-NMR (release 6.1). Bruker Daltonik GMBH, Bremen, Germany.
[11] Yeap, G. Y., Ha, S. T., Nakamura, Y., Boey, P. L., Mahmood, W. A. K., Ito, M. M., Nakai, H., & Yamaki, M. (2004). *Spectrosc. Lett.*, *37*(4), 319.
[12] Yeap, G. Y., Ha, S. T., Ito, M. M., Boey, P. L., & Mahmood, W. A. K. (2004). *J. Mol. Struct.*, *687*, 57.
[13] Demus, D. & Richter, L. (1978). *Textures of liquid crystals*, New York: Verlag Chemie.
[14] Kumar, S. (2001). *Liquid crystals: Experimental study of physical properties and phase transitions*, United Kingdom: Cambridge University Press, Cambridge.
[15] Solomons, T. W. G. (1994). *Fundamentals of organic chemistry*, New York: Wiley.